January 1, 1997

Diffraction Effects in Single- and Two-Laser Photothermal Lens Spectroscopy

Stephen E. Bialkowski, *Utah State University*
Agnes Chartier

Diffraction effects in single- and two-laser photothermal lens spectroscopy

Stephen E. Bialkowski and Agnès Chartier

A simple method for calculating the effects of optical geometry on photothermal lens signals is shown. This method is based on calculating cumulative electric-field phase shifts produced by a series of Gaussian refractive-index perturbations produced by the photothermal effect. Theoretical results are found for both pulsed-laser and continuous Gaussian laser excitation sources and both single- and two-laser apparatuses commonly employed in photothermal lens spectroscopy. The effects of apparatus geometry on the resulting signal are shown. Analytical time-dependent signal results are found for small signals. Analytical pump–probe focus geometry results allow direct optimization for certain conditions. The calculations indicate that the photothermal lens signal is, in general, optimized for near-field detection-plane geometries. © 1997 Optical Society of America

Key words: Photothermal lens spectroscopy, diffraction, beam propagation, optimization.

1. Introduction

In thermal lens spectroscopy, the heat deposited in the medium after absorption of the energy from a Gaussian laser beam by a sample creates a radially dependent temperature distribution that, in turn, produces a refractive-index gradient. In most condensed phases, because of a decrease in density with increasing temperature, the variation of the refractive index with temperature is negative and the medium behaves as a diverging lens. During lens formation, the propagation of the Gaussian beam through the sample cell is distorted and expanded. This latter effect is commonly probed by the measurement in the far field of the changes in the laser's center intensity. The probe beam can be the excitation laser itself or another continuous-wave laser. In the first theoretical treatments,[1,2] the thermally induced refractive index was assumed to be approximately parabolic near the beam axis and to behave as an ideal thin lens. These models, mostly developed for the single-laser apparatus, assume that the laser beam size remains constant as the laser beam passes through the sample cell. As the photothermal lens signal cannot be found from the Gaussian beam propagation through the sample cell, Sheldon *et al.*[3] have developed a model that takes into account the aberrant nature of the thermal lens. The thermal refractive index was approximated as a linear shift, and a diffraction integral was used to solve for the signal obtained for the single-laser photothermal lens. Approximations made in the derivations are similar to those of Fresnel or even Fraunhofer diffraction and results are valid only for the far-field detection plane or pinhole aperture placement. Results obtained from these two models were later analyzed,[4,5] and the parabolic model was found to be less accurate for a highly absorbing sample. The parabolic model was corrected to take into account the refractive shape of the lens.[4] The difference between the beam geometries when the parabolic approximation was used and those obtained with diffraction is significant, a factor 1 versus $3^{1/2}$.

The *ABCD* rule for Gaussian beam propagation has also been used to find the radial power distribution for Gaussian refractive-index perturbations under mode-matched conditions.[6,7] The same approach was used to describe the probe-beam-waist dependence on the thermal lens signal[8,9] relative to its position in the sample for dual-beam pulsed-laser excitation. Most recently, the phase-shift method has been used to calculate probe-laser irradiance profiles and photothermal thermal lens signals for nonlinear multiphoton absorption by use of the z-scan technique.[10] Similar calculations were performed by means of Fresnel diffraction integrals to find the probe-laser radial power distribution.[11–13] More re-

The authors are with the Department of Chemistry and Biochemistry, Utah State University, Logan, Utah 84322-0300.

Received 26 February 1996; revised manuscript received 6 February 1997.
0003-6935/97/276711-11$10.00/0

Table 1. Symbols Used in this Paper

Symbol	Definition (Units)	Symbol	Definition (Units)
α	Absorption coefficient (m^{-1})	r	Radius (m)
C_p	Heat capacity (J $kg^{-1}K^{-1}$)	ρ	Density (kg m^{-3})
d	Sample-to-detector distance (m)	S	Photothermal lens signal
D_T	Thermal diffusion coefficient (W m^{-2})	t	Time (s)
$\mathbf{E}$	Electric field ($W^{1/2}m^{-1}$)	$t(r, t)$	Transmission
E	Photothermal enhancement factor	t_c	Characteristic time constant (s)
$\delta\phi$	Optical phase shift (rad)	T	Temperature (K)
ϕ	On-axis phase shift (rad)	w	Gaussian beam-waist radius (m)
H	Integrated irradiance (J/m^2)	w_p	Probe-laser Gaussian beam waist (m)
k	Probe-laser wave vector (m^{-1})	Y_H	Heat yield
κ	Thermal conductivity (W $m^{-1}K^{-1}$)	z	Spatial coordinate (m)
l	Sample path length (m)	z'	Probe focus-to-sample distance (m)
λ_p	Probe-laser wavelength (m)	z_0	Confocal parameter (m)
q	Complex beam parameter (m^{-1})	$z_{0,p}$	Probe-laser confocal parameter (m)
Q	Energy (J)		

cently Shen *et al.*[14] used the Fresnel diffraction approach to calculate the photothermal lens signal obtained with the two-laser, mode-mismatched optical apparatus for continuous excitation. As in the work of Sheldon *et al.*,[3] Shen *et al.* approximated the exponential phase shift in linear terms. However, the latter is the most general of the continuous-excitation-laser results because it can be used to predict the optimum beam conditions for the two-laser apparatus.

All these reports use the same general procedure. First, the complex transmission is determined from the temperature change and the resulting refractive-index change. Second, the effect of the passage of the Gaussian probe beam through the sample is found by multiplication by the complex transmission function. Implicit here is the assumption that the sample cell is thin enough that the probe-beam radius does not change significantly as the beam passes through the sample. In diffraction, this assumption is valid when the distance between the sample cell and the detection plane is much greater than the optical path length through the cell. Third, the perturbed probe beam is progressed to the detection plane by either a diffraction integral or Gaussian beam propagation equations.

The purpose of this paper is to illustrate a straightforward method for determining the effect that a Gaussian refractive-index perturbation has on the propagation of a Gaussian probe-laser beam. The refractive-index perturbation is cast as a complex transmission element. The electric field of the probe-laser beam is found first by multiplication by the complex transmission and then modification of the complex beam parameter to account for free-space propagation. The method is simpler than using Fresnel diffraction integrals, although the results are almost equivalent. Results obtained with this method are equivalent to those obtained by the solution of Fresnel diffraction integrals to within a linear phase-shift term.[15] In this paper, a single model is developed that describes photothermal lens signals produced by both pulsed and continuous-wave excitation-laser sources. The magnitude and the time dependence of the thermal lens signal are studied relative to sample cell distance to the detection plane, and optimum beam geometries are predicted. Enhancement factors obtained under pulsed and continuous-wave excitation are also compared. The geometry of Twarowski and Kliger[16] is used to facilitate comparison with refraction theory results. The symbols used in this paper are given in Table 1.

2. Experimental Section

A 66-MHz 80486 PC with symbolic algebra software (MACSYMA, Symbolics, Inc.) is used to derive the analytical photothermal lens signals. The detailed calculation steps were recorded and stored in MACSYMA batch files to facilitate derivation and model testing. Results from symbolic derivations are written as C language code, which is easily incorporated into the graphics generation code, also written in C. Simulations are calculated with programs written in C language. Each simulation consists of a 200×200 signal magnitude versus parameter grid and takes $\sim$10 s to calculate with the analytical expressions. Surface contour shading uses cosine normal weighting for gray-tone generation. The shaded contours are plotted on a PostScript printer. Copies of the MACSYMA batch files and C language graphics code can be obtained from the authors.

3. Probe-Laser Diffraction Effects for Instantaneous Pulsed Excitation

Photothermal lens signals are calculated by first finding the time-dependent temperature change resulting from instantaneous sample excitation. Next, the radially dependent optical phase shift produced by this temperature change is found. The phase shift is subsequently used to find the effect on the probe-laser beam. The temporal impulse response is subsequently used to determine the photothermal lens signals produced from continuous excitation. This is accomplished by the integration of the impulse response over the time the continuous-excitation laser is operating. The usual assumptions used to calculate the instantaneous photothermal lens signal are used here.[16] In particular, it is assumed that the excitation pulse is of short duration relative to the time that the signal is monitored, that excited-state energy transfer is instantaneous, and that energy transfer instantly produces a density change that is inversely proportional to the temperature change. The acoustic wave generated by rapid expansion of the heated sample is not accounted for with these assumptions nor is the acoustic-relaxation-limited signal rise time. However, finite excited-state relaxation rates may be accounted for by convolution of the impulse response with the time rate of heat production.

The case of a pulsed-laser-excited sample probed with a continuous laser is examined first. The radial intensity distribution of a TEM_{00} Gaussian excitation beam can be expressed as

$$H(r) = \frac{2Q}{\pi w^2} \exp\left(\frac{-2r^2}{w^2}\right), \tag{1}$$

where $H(r)$ (in joules times inverse square meters) is the integrated irradiance, Q (in joules) is the pulse energy, w (in meters) is the excitation-beam electric-field radius, and r is the radial distance from the beam center. The instantaneous heat generated per unit length between r and $r + \mathrm{d}r$ is

$$Q(r, t) = 2\pi\delta(t)\alpha H(r) r \mathrm{d}r \tag{2}$$

where α (in inverse meters) is the exponential absorption coefficient and $\delta(t)$ is the delta function. The expression for the temperature change in the sample as a function of radius and time can be obtained by the solution of the heat transfer equation for an instantaneous source[17]:

$$\rho C_p \frac{\mathrm{d}}{\mathrm{d}t}[\delta T(r, t)] - \kappa \nabla^2[\delta T(r, t)] = Q(r, t), \tag{3}$$

where ρ (in kilograms times inverse cubic meters), C_p (in joules times inverse kilograms times inverse degrees Kelvin), and κ (in joules times inverse meters times inverse seconds times inverse degrees Kelvin) are density, specific heat, and thermal conductivity of the sample, respectively. Equation (3) has a solution given by

$$\delta T(r, t) = \int_0^t \int_0^\infty Q(r', t - t') G(r, r', t') \mathrm{d}r' \, \mathrm{d}t', \tag{4}$$

where

$$G(r, r', t) = \frac{1}{4\pi\kappa t'} \exp\left[\frac{-(r^2 + r'^2)}{4D_T t'}\right] I_0\left(\frac{rr'}{2D_T t'}\right) \tag{5}$$

is the Green's function for radial symmetric diffusion, $D_T = \kappa/\rho C_p$ (in watts times inverse square meters) is thermal diffusivity, and I_0 ( ) is the modified zero-

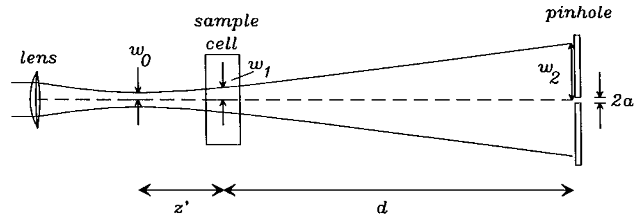

Fig. 1. Geometry that was used to define the theoretical photothermal lens signal. The probe laser enters from the left and is focused to a minimum spot radius of w_0 at a distance z' before the sample cell. It has a beam-waist radius of w_1 at the sample and w_2 at the pinhole aperture before the detector. The pinhole aperture is a distance d after the sample cell. Probe beams focused beyond the sample are indicated by negative z'.

order Bessel's function. After the integration is performed, the time-dependent temperature change is

$$\delta T(r, t) = \frac{2\alpha Q Y_H}{\pi w^2(t) \rho C_p} \exp\left[\frac{-2r^2}{w^2(t)}\right], \tag{6}$$

where Y_H is the amount of energy converted to heat, $w^2(t) = w^2(1 + 2t/t_c)$ (in square meters) is the time-dependent radius of the temperature change, and $t_c = w^2/4D_T$ is a characteristic thermal time constant of the medium.

In pulsed, TEM_{00} laser excitation, the refractive-index perturbation is radially symmetric and of Gaussian form. Assuming that the excitation-laser and the probe-laser beam waists do not change significantly through the sample, the time-dependent complex transmission $t(r, t)$ is a function of only the radius and the sample path length. The complex transmission is exponentially related to the time- and radial-dependent phase shift $\delta\phi(r, t)$. The phase shift, in turn, is the time-dependent temperature change multiplied by the thermo-optical coefficient $(\mathrm{d}n/\mathrm{d}T)$ (in inverse degrees Kelvin) and the sample path length l (in meters). Thus

$$t(r, t) = \exp[i\delta\phi(r, t)] \approx \exp\left[ikl\left(\frac{\mathrm{d}n}{\mathrm{d}T}\right)\delta T(r, t)\right],$$
$$t(r, t) \approx \exp\left\{k\left(\frac{\mathrm{d}n}{\mathrm{d}T}\right)\frac{2\alpha l Q Y_H}{\pi w^2(t)\rho C_p}\exp[-2r^2/w^2(t)]\right\}, \tag{7}$$

where $\delta\phi(r)$ is the radial-dependent phase shift, i is the square root of -1, $k = 2\pi/\lambda_p$ (in inverse meters) is the probe-laser wave vector, and λ_p (in meters) is the probe-laser wavelength.

A schematic of the geometry used to define the theoretical signal is shown in Fig. 1. The equation that describes the probe-laser electric field, focused at a distance z' (in meters) in front of the sample cell, is that of a Gaussian beam at distance z' from the focus.

Without the longitudinal phase terms, the electric field of a probe laser is

$$\mathbf{E}(r, z') = \mathbf{E}_0 \frac{q(0)}{q(z')} \exp\left[\frac{-ikr^2}{2q(z')}\right]. \tag{8}$$

The longitudinal or z-axis phase terms do not affect the probe-beam power and are neglected here in favor of simplicity. $q(z') = iz_{0,p} + z'$, $z_{0,p} = \pi w_{0,p}{}^2/\lambda_p$ is the probe-laser confocal parameter, $q(z')$ is the complex beam parameter at z' that is normally found with the inverse relationship $1/q(z') = 1/R_p(z') - i2/kw_p{}^2(z')$, where subscript p is used to indicate probe-laser parameters, $R_p(z')$ is the radius of curvature of the wave front,[18] and $w_p{}^2$ is the probe-beam radius. The electric field is $\mathbf{E}(r, z')t(r, t)$ after passing through and just beyond the sample.

In diffraction theory, we find the electric field in the detection plane, placed a distance d past the sample, by performing the integrations or Fourier transforms required in Fresnel diffraction calculations. For the rather complicated form of the phase-shift term produced by the Gaussian temperature change, integration requires some type of simplification. This simplification is accomplished by expansion of the exponential transmission in a series, as shown by Weaire *et al.*[6]:

$$t(r, t) = \exp[i\delta\phi(r)] = \sum_{m=0}^{\infty} \frac{[i\phi(t)]^m}{m!} \exp\left[\frac{-2mr^2}{w^2(t)}\right],$$
$$\phi(t) = -k\left(\frac{\mathrm{d}n}{\mathrm{d}T}\right)\frac{2\alpha lQY_H}{\pi\rho C_p w^2(t)}. \qquad (9)$$

With this definition, the negative photothermal lens generated in most samples results in a positive on-axis phase shift ϕ. Because the series expansion is a sum over Gaussian terms and because the product of two Gaussians is also a Gaussian, the electric field in the detector plane can be found by simple modification of the complex beam parameter of each Gaussian series term by use of the *ABCD* method for Gaussian beam propagation.[18] When the electric field is multiplied by the transmission, the electric field just past the sample cell is the sum

$$\mathbf{E}(r, z') = \mathbf{E}_0 \frac{q(0)}{q(z')} \sum_{m=0}^{\infty} \frac{[i\phi(t)]^m}{m!} \exp\left[\frac{-ikr^2}{2q_m(t)}\right]. \qquad (10)$$

The complex beam parameter $q_m(t)$ is a function of both excitation- and probe-laser beam waists:

$$\frac{1}{q_m(t)} = \frac{1}{R_p(z')} - i\,\frac{2}{kw_m{}^2},$$
$$\frac{1}{w_m{}^2} = \frac{1}{w_p{}^2(z')} + \frac{2m}{w^2(t)}, \qquad (11)$$

where $R_p(z') = (z_{0,p}{}^2 + z'^2)/z'$ and $kw_p{}^2(z')/2 = (z_{0,p}{}^2 + z'^2)/z_{0,p}$ are the Gaussian beam parameter definitions of the unperturbed probe laser, and the complex beam parameter for the mth series term is $1/q_m(t) = 1/q(z') - i[4m/kw^2(t)]$. Because the effect of a lens on the propagation of a Gaussian beam is found from $1/q - 1/f$, the Gaussian probe-laser beam apparently experiences a series of complex lenses of focal lengths $f = -ikw^2(t)/4m$. When the *ABCD* method is used, the complex beam parameter that describes the electric field in the detection plane some distance d past the sample cell is $q_m(t) + d$. With this rule applied to each of the terms in the series, the resulting electric field in the detection plane is

$$\mathbf{E}(r, d) = \mathbf{E}_0 \frac{q(0)}{q(z')} \sum_{m=0}^{\infty} \frac{[i\phi(t)]^m}{m!} \times \left[\frac{q_m(t)}{q_m(t) + d}\right] \exp\left\{\frac{-ikr^2}{2[q_m(t) + d]}\right\}. \qquad (12)$$

The power of the probe laser is found from the square of the electric field, $\Phi(r, d) \propto |\mathbf{E}(r, d)|^2$. This result shows that the electric field in the detection plane is a series of Gaussian beams, each with a different beam-waist radius and phase. The first term in the series describes the unperturbed probe-laser beam. Subsequent terms reflect the corrections due to the photothermal perturbation. The series will converge rapidly for small $\phi(t)$. Retaining only the first two terms is probably sufficient for describing most small photothermal lens signals.

The electric-field result shown above is similar to that obtained by Weaire *et al.*,[6] Bialkowski,[8] and Kozich *et al.*[10] However, in these studies, only the real part of the inverse complex beam parameter is retained. Here the complex electric-field amplitude is retained for each Gaussian beam so that the electric fields may cancel in the superposition. The linear phase-shift term is also neglected. Recall that there are actually two parts to the longitudinal phase shift, a linear term that depends on only the z-axis distance and a tangent term that depends on the z-axis distance and also on the confocal distance z_0.[18] Previous derivations[6,8,10] included both longitudinal phase-shift terms, in keeping with the Gaussian beam propagation solution to Maxwell's equations. With the tangent phase term, the real part of the pre-exponential term, $\Re\{[1 + d/q_m(t)]^{-1}\}$, is used.

The electric-field result is also nearly identical to that obtained with a Fresnel diffraction integral.[11,13] Again, the main difference is the linear longitudinal phase term. In fact, our approach does not explicitly account for linear longitudinal phase shift. The electric field calculated by this method can be amended to include the longitudinal phase shift by multiplication by $\exp[-i(z' + d)]$ if the phase of the electric field is important, e.g., for calculating photothermal interferometry signals. The longitudinal phase-shift term cancels in the probe power calculation used below.

Although exact, this result does not lend itself to easy interpretation. In addition to the dependence on the probe focus z' and detection plane d positions and the time-dependent photothermal perturbation strength $\phi(t)$, the diffraction result is a function of the radial offset in the detection plane r and excitation-laser and probe-laser beam-waist radii $w(t)$ and $w_{0,p}$. There is no simple way to analyze these data. We calculate the probe-laser power in the detection plane by first performing the sum over the electric field component and then by taking the complex square of the field. A discussion of the probe-laser beam profile changes is found in Ref. 13. The discussions below are restricted to the results obtained with a pinhole aperture to monitor the thermal lens signal.

4. Beam-Waist and Position Effects

Insight into how experimental geometry affects the maximum and time-dependent signals can be gained through an approximate analytical expression for the diffractive photothermal lens signal.[3] The first two terms in the series, e.g., $m = 0$ and $m = 1$, may be used to approximate the probe-laser power passing through the pinhole aperture in the detection plane. This is equivalent to approximating the exponential phase shift by $\exp(i\delta\phi) \approx 1 + i\delta\phi$.[3,14] The higher-order expansion terms are necessary for accurate signal prediction only in highly absorbing samples or when high-power excitation sources are used. Sheldon *et al.*[3] argue that because the induced phase shift in most photothermal lens experiments is much less than 1, higher-order series approximations are not necessary. Using this approximation allows an analytical expression for the probe-laser power transmitted through the pinhole aperture. When only the first two terms in the series are used and terms up to only the first order in the photothermal phase shift are retained, the relative time-dependent probe-laser power is

$$\Phi(t)/\Phi(\infty) \approx 1 - \phi(t)\,\frac{8\mathrm{d}kw^2(t)({z_{0,p}}^2 + z'^2 + \mathrm{d}z')}{k^2w^4(t)({z_{0,p}}^2 + z'^2 + 2\mathrm{d}z' + d^2) + 8kw^2(t)d^2z_{0,p} + 16d^2({z_{0,p}}^2 + z'^2)}, \tag{13}$$

where $\Phi(t)$ (in watts) is the probe-laser power passing through a pinhole aperture at $r = 0$.

5. Far-Field Detection Plane

If the detector–pinhole plane is in the far field, then

$$\lim_{d\to\infty} \Phi(t)/\Phi(\infty) \approx 1 - \phi(t) \times \frac{8kw^2(t)z'}{k^2w^4(t) + 8kw^2(t)z_{0,p} + 16({z_{0,p}}^2 + z'^2)}. \tag{14}$$

The photothermal lens signal is calculated from the power ratio. A simple expression for the time-dependent signal is found with the assumption that $\phi z' \ll z_{0,p}$ and $|z'| \ll |z_{0,p}|$ in the denominator of the signal expression. With these assumptions, the photothermal lens signal[16] is

$$S_{\text{pulsed}}(t) = \frac{\Phi(t) - \Phi(\infty)}{\Phi(t)} \approx \frac{2z'}{f_{\text{pulsed}}(0)}\,\frac{1}{(1 + 2{w_{0,p}}^2/w^2 + 2t/t_c)^2}, \tag{15}$$

where $1/f_{\text{pulsed}}(0) = 4\phi(0)/kw^2$ is the definition for the initial pulsed-laser photothermal lens focal length predicted from refractive optics theory:

$$f_{\text{pulsed}}{}^{1}(0) = \left(\frac{\mathrm{d}n}{\mathrm{d}T}\right)\frac{8\alpha lY_HQ}{\pi w^4\rho C_p}. \tag{16}$$

This approximate result is similar to that predicted with refraction optics under the same conditions, $2z'/f_{\text{pulsed}}(0)(1 + 2t/t_c)^2$. In fact, when the probe-laser beam waist $w_{0,p}$ is much smaller than that of the excitation source, the diffraction and refraction methods yield equivalent results. This may be expected because the probe laser passes through the index perturbation near the axis when $w_{0,p} \ll w$ and the refractive lens is based on the on-axis, i.e., $r = 0$, curvature of the perturbation.[1] For finite probe-beam radii, the maximum $t = 0$ signal will be a factor of $w^2/(w^2 + 2{w_{0,p}}^2)$ smaller than that predicted by refraction. These results are in keeping with our earlier diffraction-optics-based signal calculations.[8]

The probe-laser beam focus position resulting in optimum signal can be obtained by the maximization of the initial photothermal lens signal with respect to z'. The resulting optimum focus position is $z'_{\text{opt}} = \pm z_{0,p}(1 + w^2/2{w_{0,p}}^2)$. The optimum initial photothermal lens signal can be found when this result is substituted into the signal equation and the terms that are linear in ϕ are retained:

$$S_{\text{pulsed,opt}}(t) = \pm\left(\frac{\mathrm{d}n}{\mathrm{d}T}\right)\frac{8\alpha lQY_H}{\lambda_p\rho C_p} \times \frac{(2{w_{0,p}}^2 + w^2)}{[2{w_{0,p}}^2 + w^2(1 + 2t/t_c)]^2 + (2{w_{0,p}}^2 + w^2)^2}, \tag{17}$$

and the zero-time (maximum) signal is

$$S_{\text{pulsed,opt}}(0) = \pm\left(\frac{\mathrm{d}n}{\mathrm{d}T}\right)\frac{4\alpha lQY_H}{\lambda_p\rho C_p(2{w_{0,p}}^2 + w^2)}. \tag{18}$$

This result explicitly shows how the probe-laser beam-waist radius affects the photothermal lens signal. The signal is apparently maximized as both the excitation and the probe-laser beams are more tightly focused. Also of interest is that the maximum optimum signal is predicted to be inversely proportional to w^2, not w^4 as in the refraction result. The maximum is also inversely proportional to λ_p. Thus tightly focused short-wavelength probe lasers should be used with a far-field detection-plane apparatus. The refraction optics approach predicts that decreasing the excitation-laser beam waist always increases the signal. The results obtained above show that this is true only to a point. If the excitation-laser beam waist is smaller than that of the probe, then no further signal improvement will be obtained.

6. Near-field detection plane

A detector-plane position is found by maximization of approximation (13) with respect to d by use of differential methods. This results in an optimum detection-plane position of $d_{\mathrm{opt}} = kw^2({z_{0,p}}^2 + z'^2)/[4{z_{0,p}}^2 + kw^2(z_{0,p} - z') + 4z'^2]$. Substitution of d_{opt} into the initial photothermal equation, followed by z' optimization, yields $z' = 0$. The optimum photothermal lens signal obtained for this geometry is

$$S_{\mathrm{pulsed,opt}}(t) = \left(\frac{\mathrm{d}n}{\mathrm{d}T}\right) \frac{8\alpha l Q Y_H}{\lambda_p \rho C_p} \frac{{w_{0,p}}^2}{w^2} \frac{(2{w_{0,p}}^2 + w^2)}{(1 + 2t/t_c)^2(2{w_{0,p}}^4 + 2w^2{w_{0,p}}^2 + w^4) + 2(2t/t_c + 1)w^2{w_{0,p}}^2 + 2{w_{0,p}}^4}, \qquad (19)$$

and the maximum zero-time signal is

$$S_{\mathrm{pulsed,opt}}(0) = \left(\frac{\mathrm{d}n}{\mathrm{d}T}\right) \frac{8\alpha l Q Y_H}{\lambda_p \rho C_p} \frac{{w_{0,p}}^2}{w^2} \frac{1}{(2{w_{0,p}}^2 + w^2)}. \qquad (20)$$

Although similar to that obtained for the far-field detection plane, the near-field signal is optimized for $w \ll w_{0,p}$, i.e., for small excitation-beam-waist radiuses. This trend was previously deduced from numerical simulations based on the Fresnel diffration integral approach.[13] However, it is difficult to find optimum geometries with a numerical simulation approach. The results obtained here explicitly show the conditions for optimization and give the resulting time-dependent signal. For a small excitation-laser beam radius,

$$\lim_{w \to 0} S_{\mathrm{pulsed,opt}}(0) = \left(\frac{\mathrm{d}n}{\mathrm{d}T}\right) \frac{4\alpha l Q Y_H}{\lambda_p \rho C_p w^2}. \qquad (21)$$

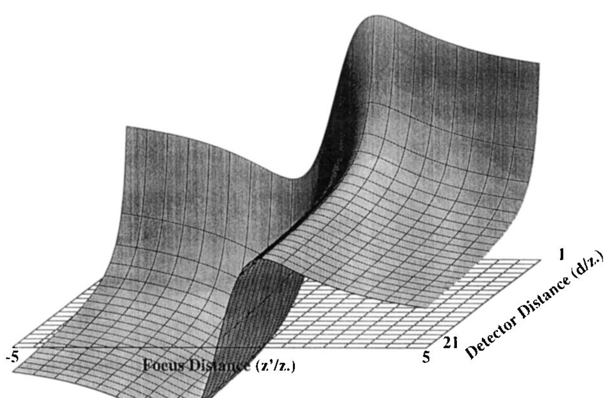

Fig. 2. Pulsed-laser-excited photothermal lens signal predicted from diffraction theory as a function of the probe-laser beam geometry. The excitation-laser beam waist was 20 μm in the sample. The minimum 632.8-nm probe-laser beam radius was 100 μm. The photothermal perturbation was small, and the signal was defined in the usual fashion.

This is in contrast to the far-field signal, which is maximized when both the excitation-laser and the probe-laser beam waists are minimized.

7. Model Calculations and Experimental Optimization

Optimum geometries obtained with differential methods must be checked to ensure that the maxima are indeed found. The signal can also change dramatically with small errors in the optical design if the optimum is sought. In either case, it is important to examine the signal as a function of the geometric parameters in order to gain insight into the optimum apparatus geometry. It is also difficult to compare signal magnitudes of the far- and the near-field detection planes from the analytical equations alone because the ratio of the respective optimum theoretical signals is proportional to a ratio of excitation- and probe-beam radii, $S_{\mathrm{near}}/S_{\mathrm{far}} = 2{w_{0,p}}^2/w^2$. Either detection geometry can be optimized relative to the other. Of primary concern are the effects of the relative distances of the probe-laser focus, the distance to the detection plane, and the relative probe-laser beam-waist radii.

First, photothermal lens signals calculated for an excitation-beam waist greater than approximately five probe-beam waists are identical to those predicted by the refraction equation.[16] Only when the probe-laser beam waist becomes of the order of, or greater than, the pump waist does diffraction theory need to be used. Shown in Fig. 2 are results of a calculation for the relative photothermal lens signal for such a case. In this plot the pulsed-laser excitation-beam radius is $w = 20$ μm and a probe-laser beam waist is $w_{0,p} = 100$ μm. These beam-waist radii will favor near-field detection. The probe-laser wavelength is 632.8 nm and the confocal distance is $z_{0,p} = 5$ cm. A photothermal phase shift of $\phi(t) = 10^{-5}$ is used because most samples have negative thermo-optical coefficients. For the plots shown here, the series was summed up to the twentieth power term. This is not usually necessary because convergence typically occurs with two to three terms. The plot is oriented with the detection-plane distance increasing toward the viewer. The probe-laser focus position varies across the surface. The $d = 0$ point was not plotted. The theoretical signal is found to be zero at this point, independent of the z' distance. In addition, near-field points with $d \leq w_p$ are of questionable value because of the small-angle approximation implicit in these results.

The signal behavior predicted by this example calculation is clearly different from that predicted by the refractive lens theory. In refraction theory, the signal levels off with increasing detection-plane dis-

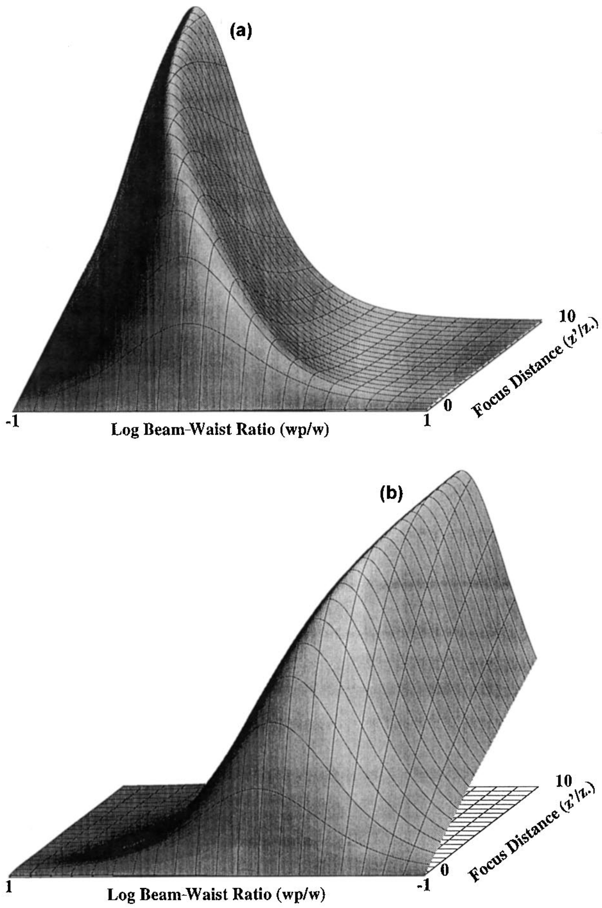

Fig. 3. (a) Far-field diffraction theory predictions for the pulsed-laser-excited photothermal lens signal as a function of the relative probe-laser beam-waist radius and focus position. The detector plane was at $d = 10$ m, the excitation beam radius was 100 μm in the sample, and the perturbation was small (10^{-5}). (b) The conditions are the same as in (a). This view is given to allow inspection of the predicted surface. The line on the right-hand side is equivalent to that predicted from refractive optics.

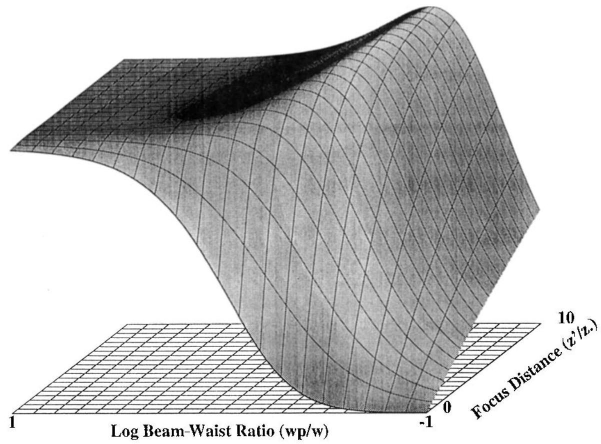

Fig. 4. Near-field diffraction theory predictions for the pulsed-laser-excited photothermal lens signal as a function of the relative probe-laser beam-waist radius and focus position. The detection plane is at $d = 5$ cm in this case. All other parameters are the same as those in Fig. 3.

tance. In contrast, the signal calculated with the equations derived here decreases with detection-plane distance. With the detection plane near the sample cell, the signal is initially positive for negative z', indicating a decrease in probe-laser power with the formation of the photothermal lens. This is only because the focus position of the probe beam is beyond the detection plane. In fact, the same behavior can be seen in Fig. 2 for the refractive lens theory. For detection-plane distances far from the sample cell, the signal exhibits a sigmoidal dependence on probe-laser beam focus position. This is in contrast to the refraction theory in which the signal is approximately proportional to z at large d. The sigmoidal dependence is similar to that observed by Berthoud *et al.*,[19] although they used a chopped excitation laser. However, the maximum calculated diffraction signal occurs at $z' \approx z_0$, not $\sim\sqrt{3}z_0$ for this set of calculation parameters.

Figures 3(a) and 3(b) illustrate the effect of the relative probe-laser beam waist on the theoretical pulsed-laser-excited photothermal lens signal. In this case the detection plane is fixed at a distance of 10 m, i.e., far field, and the probe-laser focus position is in front of the sample. The relative minimum probe-laser beam-waist radius varies logarithmically from a factor of 0.1–10 of that of the excitation beam. The excitation-beam-waist radius is 100 μm, the probe-laser wavelength is 632.8 nm, and the phase shift is 10^{-5}. The figures span a range from that adequately predicted by refraction theory to a range within which diffraction must be used. It is interesting to note that the diffraction result reproduced the trends predicted from refractive optics in the appropriate region. A maximum in signal strength appears for probe-beam-waist radii slightly less than that of the excitation source. Whether or not this indicates a trend can be addressed only by examination of the effects of detection-plane position. Figures 3(a) and 3(b) also show that there is no single probe-laser beam focus position that optimizes the signal. Apparently there is no best z'/z_0 for pulsed-laser-excited photothermal lens signals predicted by diffraction.

Figure 4 shows the calculated photothermal lens signal response for the near-field condition of $d = 5$ cm. Of interest here is the apparent flat signal region for a large probe-beam waist. In combination with the trends shown in Fig. 2, in which it is shown that the signal increases with decreasing sample-to-detection-plane distance, it would seem that a stable optical configuration for pulsed-laser-excited photothermal lensing is one in which a relatively large probe laser is focused several $z_{0,p}$ in front of the sample and the detection plane is close to the sample. The latter can be accomplished when the unfocused probe laser is placed close to the sample.[13] However, this configuration does not result in the maximum signal. Figure 4 shows that the maximum signal is obtained for probe beams focused outside the sample cell and for w_p slightly smaller than w.

8. Probe-Laser Diffraction Effects for Continuous Excitation

The time integral of the Green's function result for a pulsed Gaussian source yields the temperature change produced for continuous-laser excitation when the term $\delta(t)H(t)$ is replaced with irradiance $E(t)$. Because the photothermal phase shift is proportional to temperature, the complex transmission for continuous excitation can be obtained by time integration of the phase-shift term in Eqs. (9):

$$t(r, t) = \exp\left[i\int_0^t \delta\phi(r, t')\mathrm{d}t'\right] = \sum_{m=0}^{\infty} \frac{i^m}{m!}\left\{\int_0^t \phi(t')\exp\left[\frac{-2r^2}{w^2(t')}\right]\mathrm{d}t'\right\}^m. \quad (22)$$

The probe-laser beam electric field may be found in the same fashion as in the pulsed-excitation case. However, terms with $m \geq 2$ are difficult to evaluate. Again, the linear phase-shift approximation $\exp(i\delta\phi) \approx 1 + i\delta\phi$ is used to simplify the results. When terms up to only first order in the photothermal phase shift are retained, the electric field at the detector plane is

$$\mathbf{E}(r, d) \approx \mathbf{E}_0 \frac{q(0)}{q(z' + d)} + \mathbf{E}_0 \frac{q(0)}{q(z')} \int_0^t i\phi(t')\left[\frac{q_1(t')}{q_1(t') + d}\right] \times \exp\{-ikr^2 2[q_1(t') + d]\mathrm{d}t'\}. \quad (23)$$

For the pinhole detection scheme used in photothermal lens spectroscopy, the integral is tractable because the radius is zero and thus the exponential term is unity. With a little algebra, the integrals can be rewritten in terms of the integration variable $T = 1 + 2t/t_c$:

$$\mathbf{E}(0, d) \approx \mathbf{E}_0 \frac{q(0)}{q(z' + d)} + \mathbf{E}_0 \frac{q(0)}{q(z')} \frac{t_c}{2} i\phi(0) \int_1^{1+2t/t_c} \times T^{-1} \frac{q(z')T - i4/kw^2}{[q(z') + d]T - i4/kw^2}\,\mathrm{d}T. \quad (24)$$

The probe-laser power ratio is formulated before the integration over time is performed:

$$\frac{\Phi(t)}{\Phi(0)} - 1 \approx \frac{t_c\phi}{2} \int_1^{1+2t/t_c} \left\{\frac{iq(z' + d)}{q(z')} \times T^{-1} \frac{q(z')T - i4/kw^2}{[q(z') + d]T - i4/kw^2} + \text{c.c.}\right\}\mathrm{d}T, \quad (25)$$

where c.c. is the complex conjugate of the first term. The probe-laser power ratio for continuous excitation is

$$\frac{\Phi(t)}{\Phi(0)} \approx 1 + t_c\phi \tan^{-1}\left\{\frac{kw^2[{z_{0,p}}^2 + (z' + d)^2] + 4d^2 z_{0,p}}{4d({z_{0,p}}^2 + z'^2 + dz')}\right\} - t_c\phi \tan^{-1} \times \left\{\frac{kw^2(1 + 2t/t_c)[{z_{0,p}}^2 + (z' + d)^2] + 4d^2 z_{0,p}}{4d({z_{0,p}}^2 + z'^2 + dz)}\right\}. \quad (26)$$

Sheldon *et al.*[3] calculated only the far-field result. The above result gives the relative power change for any set of experimental parameters. In continuous-laser-excited photothermal lens spectrometry, the maximum signal is reached for a long irradiation time. Taking the limit as time approaches infinity and calculating the signal in the usual fashion result in the signal expression

$$S_{\mathrm{cw}}(\infty) = \frac{\Phi(0) - \Phi(\infty)}{\Phi(\infty)} \approx \frac{1}{1 - t_c\phi \tan^{-1}\left\{\dfrac{4d({z_{0,p}}^2 + z'^2 + dz')}{kw^2[{z_{0,p}}^2 + (z' + d)^2] + 4d^2 z_{0,p}}\right\}} - 1. \quad (27)$$

The signal magnitude is a function of the $t_c\phi$ product. This product can be represented in several forms:

$$-t_c\phi = \frac{w^2\rho C_p}{4\kappa} k\left(\frac{\mathrm{d}n}{\mathrm{d}T}\right)\frac{2\alpha l \Phi_0 Y_H}{\pi\rho C_p w^2} = \left(\frac{\mathrm{d}n}{\mathrm{d}T}\right)\frac{\alpha l \Phi_0 Y_H}{\lambda_p \kappa} = \frac{\lambda}{\lambda_p}\frac{z_0}{f_{\mathrm{cw}}(\infty)}, \quad (28)$$

where $f_{\mathrm{cw}}(\infty)$ is the focal length of the thermal lens at infinite time, produced by continuous-laser excitation and calculated in the usual fashion, i.e., from the second derivative of radial refractive-index change distribution with respect to r. The last expression shows the relationship to the inverse focal length calculated from refractive optics theory. This connection may be used to make adjustments to the result, for example, in the case in which the effective sample path length is limited by the beam divergence of the excitation laser.

The continuous-laser-excited photothermal lens signal magnitude is plotted in Fig. 5 for a case in which the probe-laser beam waist is much larger than that of the excitation source. Parameters used to generate this plot are the same as those of Fig. 2, with the exception that here the magnitude term is $t_c\phi = -(\mathrm{d}n/\mathrm{d}T)\alpha/\Phi_0 Y_H/\lambda_p\kappa$. Signals above the plane correspond to a decrease in probe power and those below correspond to an increase in power. For

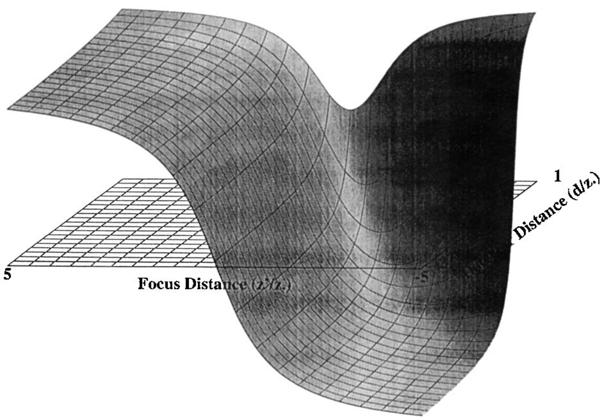

Fig. 5. Continuous-laser-excited photothermal lens signal predicted from diffraction theory. The signal magnitude is defined by $[\Phi(\infty) - \Phi(0)]/\Phi(0)$. The excitation-laser beam waist is 20 μm and the 632.8-nm laser beam waist is 100 μm. The signal is apparently maximum at small detection-plane distances.

detector-plane positions near the sample, only positive signals result. This is because the negative focal length of the thermal lens causes blooming of the probe beam. As the detector plane is moved away from the sample, the signal can be positive or negative, depending on whether the probe laser was focused in front of or beyond the sample. Within the range of parameters used in this model calculation, a maximum signal occurs for near-field conditions, e.g., $d = z_{0,p}$ and $z' = \pm 5z_{0,p}$. When this plot is compared with that for pulsed-laser excitation, it is apparent that the signal varies more slowly with z' in the far field. In fact, the behavior is similar to that predicted by refraction theory for probe focus positions within $\pm z_{0,p}$. The reason for this may be that the continuous-laser-excited photothermal perturbation is broader than the initial perturbation generated with a pulsed source. One final feature of this plot that should be noted is the apparent lack of a signal maximum with respect to z' position. This is confirmed by examination of the differential with respect to z'. Apparently the continuous-laser-excited photothermal lens signal is optimized for large probe-beam focus positions, but there is no one best probe-laser focus position.

The relative power resulting from probe-beam diffraction may also be compared with the previous studies of diffraction effects in two-laser, continuous-excitation photothermal lens spectroscopy. To compare this with previous results, the detection plane is taken to be far from the sample cell. For this geometry the resulting power is

$$\lim_{d\to\infty} \frac{\Phi(t)}{\Phi(0)} \approx 1 + t_c\phi \tan^{-1}\left(\frac{kw^2 + 4z_{0,p}}{4z'}\right) - t_c\phi \tan^{-1}\left[\frac{kw^2(1 + 2t/t_c) + 4z_{0,p}}{4z'}\right]. \quad (29)$$

This result also leads to a compact expression for the maximum probe-laser power change that would occur for infinitely long excitation-laser irradiation times. In this case,

$$\frac{\Phi(\infty)}{\Phi(0)} - 1 \approx -t_c\, \phi \tan^{-1}\left[\frac{4z'}{k(w^2 + 2w_{0,p}{}^2)}\right]. \quad (30)$$

It is interesting that the two-laser apparatus appears to be linear in absorbed energy $t_c\phi$ when the photothermal lens signal is defined by $[\Phi(\infty) - \Phi(0)]/\Phi(0)$. This expression also shows the signal dependence on the excitation-laser and probe-laser beam-waist radii. Decreasing either of these will enhance the photothermal lens signal detected in far field for a given z', with the caveat that decreasing the excitation-laser beam waist may decrease the effective path length through the sample.

9. Diffraction Effects for a Single-Laser Photothermal Lens

Diffraction results for a single-laser photothermal apparatus can be found from the continuous-excitation two-laser case by simply equating excitation-laser and probe-laser beam parameters. Sheldon *et al.*[3] introduced a different way to define the continuous-laser-excited photothermal lens signal that yields a more compact result for diffraction theory. They defined the time-dependent signal as a ratio of the power change to that which occurs at infinite time. With this definition, the time-dependent photothermal lens signal obtained in the far field is

$$S_{\mathrm{cw}}(t) = \frac{\Phi(t) - \Phi(\infty)}{\Phi(\infty)} = \frac{t_c\phi \tan^{-1}\left[\dfrac{4z'}{kw^2(1 + 2t/t_c) + 4z_0}\right]}{1 - t_c\phi \tan^{-1}\left(\dfrac{4z'}{kw^2 + 4z_0}\right)}. \quad (31)$$

z_0 is used here because there is no distinction between the excitation and the probe lasers in the single-laser photothermal lens apparatus. For the mode-matched conditions of a single-laser experiment, w and z_0 are related. By first substituting $w_0{}^2(1 + z'^2/z_0{}^2)$ for w^2, where w_0 is the minimum beam-waist radius of the Gaussian excitation source, then using the definition for $z_0 = kw_0{}^2/2$, we find that the far-field signal for the single-laser apparatus is

$$S_{\mathrm{cw}}(t) = \frac{t_c\phi \tan^{-1}\left\{\dfrac{2z'/z_0}{(z'/z_0)^2 + 3 + 2[(z'/z_0)^2 + 1]t/t_c}\right\}}{1 - t_c\phi \tan^{-1}\left[\dfrac{2z'/z_0}{(z'/z_0)^2 + 3}\right]}. \quad (32)$$

With this signal definition, the maximum power change is

$$S_{\mathrm{cw}}(0) = \frac{1}{1 - t_c\phi \tan^{-1}\left[\dfrac{2z'/z_0}{(z'/z_0)^2 + 3}\right]} - 1. \quad (33)$$

It is straightforward to show by derivative methods that the maximum signal will occur when $z' = \pm\sqrt{3}z_0$.

10. Effect of Diffraction on the Thermal Lens Enhancement Factor

The photothermal lens enhancement factor introduced by Dovichi and Harris[20] is a figure of merit that may be used to gauge photothermal spectroscopy to conventional absorption spectrophotometry. It is the ratio of the photothermal lens signal to the change in power observed by use of absorption spectrophotometry for small absorbance samples. The enhancement factor is equal to the signal-to-noise ratio improvement (or degradation) obtained with photothermal lens spectroscopy, assuming that both spectroscopies are limited by equivalent noise sources. For small optical absorbance, the exponential power dependence $\Phi = \Phi_0 \exp(-\alpha l)$, where Φ_0 is the power at the sample and Φ is the transmitted power, may be approximated by a Taylor series. With the first two series terms retained, $\Phi \simeq \Phi_0(1 - \alpha l)$ and the power ratio is $(\Phi_0 - \Phi)/\Phi_0 \simeq \alpha l$. This absorption spectrophotometry signal is similar in form to that defining the photothermal lens spectroscopy signal, i.e., a relative power change. The photothermal lens enhancement factor is thus equal to the photothermal lens signal divided by the αl product.

The pulsed-laser-excited diffraction results can be used to determine the theoretical photothermal lens enhancement factor for a variety of excitation-laser and probe-laser focusing geometries. The enhancement based on the far-field result can be compared with that obtained with the refraction-based theory, as the enhancement is usually calculated for large d in this case. For example, optimizing with respect to probe-laser focus position $z' = \pm z_{0,p}(1 + w^2/2w_{0,p}{}^2)$ gives an optimum enhancement factor of

$$E_{\text{pulsed,opt}} = \left|\left(\frac{\mathrm{d}n}{\mathrm{d}T}\right)\right| \frac{4QY_H}{\lambda_p \rho C_p (2w_{0,p}{}^2 + w^2)}. \qquad (34)$$

The enhancement is a function of the minimum beam-waist radius of both lasers. However, the enhancement factor is inversely proportional to the probe-laser wavelength.

If the optics of the apparatus are restrained to have excitation-laser and probe-laser beam waists equal at the focus, i.e., mode matched, then the enhancement found from approximation (14) is

$$E_{\text{pulsed}} \approx \left|\left(\frac{\mathrm{d}n}{\mathrm{d}T}\right)\right| \frac{3^{1/2}QY_H}{\lambda w^2 \rho C_p}. \qquad (35)$$

This result can be directly compared with the theoretical enhancement obtained with refraction optics for mode-matched beams: Both are inversely proportional to the excitation-laser wavelength. The diffraction result shown above is a factor of 1/3 less than that previously reported, which was obtained with a refractive optics approach.[21]

The optimum near-field detector-plane pulsed-laser enhancement is readily found:

$$E_{\text{pulsed,opt}} = \left|\left(\frac{\mathrm{d}n}{\mathrm{d}T}\right)\right| \frac{8QY_H}{\lambda_p \rho C_p} \frac{w_{0,p}{}^2}{w^2} \frac{1}{(2w_{0,p}{}^2 + w^2)}. \qquad (36)$$

As with the mode-matched geometry result, the enhancement increases with decreasing excitation-beam-waist radius.

When the two-laser continuous-excitation signal for the detector plane placed in the far-field is defined as in approximation (29) and the optical phase-shift term is substituted, the maximum signal found for long times is

$$S_{\text{cw}}(\infty) = \left(\frac{\mathrm{d}n}{\mathrm{d}T}\right) \frac{\alpha l \Phi_0 Y_H}{\lambda_p \kappa} \tan^{-1}\left[\frac{4z'}{k(w^2 + 2w_{0,p}{}^2)}\right]. \qquad (37)$$

As implied by the results illustrated in Fig. 5, this signal does not exhibit an optimum z'. A maximum signal occurs when the argument of the arctangent function is infinite. Assuming that $z' \gg k(w^2 + 2w_{0,p}{}^2)$, the arctangent function is $\sim\pi/2$ and the photothermal lens enhancement factor is

$$E_{\text{cw}}(\infty) = \left|\left(\frac{\mathrm{d}n}{\mathrm{d}T}\right)\right| \frac{\pi \Phi_0 Y_H}{2\lambda_p \kappa}. \qquad (38)$$

The implication here is that the excitation laser is focused into the sample in order to obtain a negligibly small beam radius and that $z' \gg z_{0,p}$.

The enhancement for single-laser excitation is easier to predict since the beam geometry for optimum signal is fixed. The optimum single-laser photothermal lens signal shown in Section 9 for far-field detection is

$$S_{\text{cw,max}} = \frac{\Phi(0) - \phi(\infty)}{\phi(\infty)} = \frac{\frac{\pi}{6} t_c \phi}{1 - \frac{\pi}{6} t_c \phi}. \qquad (39)$$

For small thermal perturbations, the term $\pi t_c \phi/6$ is much less than 1 and can be neglected in the denominator. The continuous, single-laser photothermal lens enhancement factor E_{cw} is

$$E_{\text{cw}} = \frac{\frac{\pi}{6} t_c \phi}{\alpha l} = \left|\left(\frac{\mathrm{d}n}{\mathrm{d}T}\right)\right| \frac{\pi \Phi_0 Y_H}{6\lambda\kappa}, \qquad (40)$$

which is a factor of $\pi/6 \approx 0.523$ of the enhancement factor obtained from refractive optics theory. Before the development of the diffraction theory, experimental determination of the enhancement factor fell short of that predicted by refraction. The diffraction theory result explains why this was observed.[5]

11. Summary

In summary, a convenient method for determining diffraction effects in photothermal lens spectroscopy has been outlined in this paper. Using the *ABCD* method for propagation of Gaussian beams resulting from the aberrant photothermal lens results in signal equations that are equivalent to those obtained with the more complicated diffraction approach. These results are explored in terms of how they affect the design of a photothermal lens apparatus for a number of different experiment designs. The method can be used to predict the optimum optical geometries for both pulsed-laser and continuous-excitation-laser experiments.

This research was supported in part by the U.S. National Institute of Health (P41RR06030). A. Chartier thanks the Laboratoire des Sciences Analytiques, Unité de Recherche Associée au Centre National de la Recherche Scientifique 435. Villeurbanne, France, for granting a sabbatical.

References

1. J. P. Gordon, R. C. Leite, R. S. Moore, S. P. Porto, and J. R. Whinnery, "Long-transient effects in lasers with inserted liquid samples," J. Appl. Phys. **36,** 3–8 (1965).
2. C. Hu and J. R. Whinnery, "New thermo-optical method and a comparison with other methods," Appl. Opt. **12,** 72–79 (1973).
3. S. J. Sheldon, L. V. Knight, and J. M. Thorne, "Laser-induced thermal lens effect: a new theoretical model," Appl. Opt. **21,** 1663–1669 (1982).
4. C. A. Carter and J. M. Harris, "Comparison of models describing the thermal lens effect," Appl. Opt. **23,** 476–481 (1984).
5. T. Higashi, T. Imasaka, and N. Ishibashi, "Thermal lens spectrophotometry with argon laser excitation source for nitrogen dioxide determination," Anal. Chem. **55,** 1907–1910 (1983).
6. D. Weaire, B. S. Wherrett, D. A. B. Miller, and S. D. Smith, "Effect of low power nonlinear refraction on laser-beam propagation in InSb," Opt. Lett. **4,** 331–333 (1979).
7. M. Sheik-Bahae, A. A. Said, and E. W. Van Stryland, "High-sensitivity, single-beam n_2 measurements," Opt. Lett. **14,** 955–957 (1989).
8. S. E. Bialkowski, "Photothermal lens aberration effects in two laser thermal lens spectrophotometry," Appl. Opt. **24,** 2792–2796 (1985).
9. J. Castillo, V. P. Kozich, and A. Marcano, "Thermal lensing resulting from one- and two-photon absorption studied with a two-color time-resolved *Z* scan," Opt. Lett. **19,** 171–173 (1994).
10. V. P. Kozich, A. Marcano, F. E. Hernandez, and J. A. Castillo, "Dual-beam time-resolved Z-scan in liquids to study heating due to linear and nonlinear light absorption," Appl. Spectrosc. **48,** 1506–1512 (1994).
11. J. Slaby, "Calculation of probe beam diffraction at laser induced thermal lens," Opt. Commun. **60,** 133–138 (1986).
12. J. Slaby, "Background illumination filtering in thermal lens spectroscopy," Anal. Chem. **61,** 2496–2499 (1989).
13. J. F. Power, "Pulsed mode thermal lens effect detection in the near field via thermally induced probe beam spatial phase modulation: a theory," Appl. Opt. **29,** 52–62 (1990).
14. J. Shen, R. D. Lowe, and R. D. Snook, "A model for CW laser induced mode-mismatched dual beam thermal lens spectrometry," Chem. Phys. **165,** 385–396 (1992); J. Shen, A. J. Soroka, and R. D. Snook, "A model for cw laser induced mode-mismatched dual-beam thermal lens spectrometry based on probe beam image detection," J. Appl. Phys. **78,** 700–708 (1995).
15. S. E. Bialkowski, *Photothermal Spectroscopy Methods for Chemical Analysis* (Wiley, New York, 1996), Chap. 4.
16. A. J. Twarowski and D. S. Kliger, "Multiphoton absorption spectra using thermal blooming. I. Theory," Chem. Phys. **20,** 253–258 (1977).
17. H. S. Carlaw and J. C. Jaeger, *Conduction of Heat in Solids*, 2nd ed. (Clarendon, Oxford, 1959).
18. A. Yariv, *Introduction to Optical Electronics*, 3rd ed. (Holt, Rinehart & Winston, New York, 1985).
19. T. Berthoud, N. Delorme and P. Mauchien, "Beam geometry optimization in dual-beam thermal lensing spectrometry," Anal. Chem. **57,** 1216–1219 (1985).
20. N. J. Dovichi and J. M. Harris, "Laser induced thermal lens effect for calorimetric trace analysis," Anal. Chem. **51,** 728 (1979).
21. K. Mori, T. Imasaka, and N. Ishibashi, "Thermal lens spectrophotometry based on pulsed laser excitation," Anal. Chem. **54,** 2034–2038 (1982).